

Received: 2016.09.07
Accepted: 2016.10.26
Published: 2017.05.23

Clinical Value and Prospective Pathway Signaling of MicroRNA-375 in Lung Adenocarcinoma: A Study Based on the Cancer Genome Atlas (TCGA), Gene Expression Omnibus (GEO) and Bioinformatics Analysis

Authors' Contribution:

Study Design A
Data Collection B
Statistical Analysis C
Data Interpretation D
Manuscript Preparation E
Literature Search F
Funds Collection G

AB 1 Ting-qing Gan
BC 2 Wen-jie Chen
CD 2 Hui Qin
E 3 Su-ning Huang
CD 1 Li-hua Yang
DF 3 Ye-ying Fang
DF 3 Lin-jiang Pan
G 2 Zu-yun Li
A 2 Gang Chen

1 Department of Medical Oncology, First Affiliated Hospital of Guangxi Medical University, Nanning, Guangxi, P.R. China
2 Department of Pathology, First Affiliated Hospital of Guangxi Medical University, Nanning, Guangxi, P.R. China
3 Department of Radiology, First Affiliated Hospital of Guangxi Medical University, Nanning, Guangxi, P.R. China

Corresponding Authors: Lin-jiang Pan, e-mail: 67666795@qq.com; Zu-yun Li, e-mail: lizuyun8877@aliyun.com

Source of support: The study was supported by the Scientific Research Project of the Basic Ability Promoting for Middle Age and Youth Teachers of Guangxi Universities (KY2016YB077) and Natural Science Foundation of Guangxi, China (2015GXNSFAA139213, 2016GXNSFAA380255)

Background: Lung adenocarcinoma (LUAD) is the most frequent lung cancer. MicroRNAs (miRNAs) are believed to have fundamental roles in tumorigenesis of LUAD. Although miRNAs are broadly recognized in LUAD, the role of miRNA-375 in LUAD is still not fully elucidated.


Material/Methods: We evaluated the significance of miR-375 expression in LUAD by using analysis of a public dataset from the Cancer Genome Atlas (TCGA) and Gene Expression Omnibus (GEO) database and a literature review. Furthermore, we investigated the biological function of miR-375 by gene ontology enrichment and target prediction analysis.

Results: MiR-375 expression was significantly higher in LUAD by TCGA data compared to normal lung tissue ($p < 0.0001$). In addition, a common pattern of upregulation for miR-375 in LUAD was found in our review of the literature. A total of 682 genes, both LUAD-related and miR-375-related, were obtained from the analytical integration. Critical pathways were unveiled in the network analysis of the overlaps, such as pentose and glucuronate interconversions, ascorbate and aldarate metabolism, and starch and sucrose metabolism. Furthermore, we identified covert miR-375 associated genes that might participate in LUAD by network analysis, such as FGF2 (fibroblast growth factor 2), PAX6 (paired box 6), and RHOJ. The expression of these three genes were all downregulated in LUAD. Finally, FGF2 was revealed to be negatively correlated with miR-375 in LUAD ($r = -0.1821$, $p = 0.0001$).

Conclusions: Overall, our study provides evidence that miR-375 is essential for the progression of LUAD.

MeSH Keywords: Carcinoma, Non-Small-Cell Lung • Computational Biology • MicroRNAs

Full-text PDF: <http://www.medscimonit.com/abstract/index/idArt/901460>

 2520

 6

 10

 40



Background

Lung cancer, an extremely heterogeneous disease, accounts for almost a quarter of cancer-related deaths [1]. Lung adenocarcinoma (LUAD) is the most aggressive histological type of lung cancer. The incident of LUAD has been increasing rapidly [2]. Unfortunately, LUAD mortality has not significantly decreased owing to the lack of early detection and lack of more effective therapies at earlier disease stages. Therefore, insights into the mechanisms of LUAD are considered urgent.

MicroRNAs (miRNAs or miRs), typically 18–23 nucleotides in length, have gained much attention as oncogenes or suppressors modulating gene activity at the post-transcriptional and translational levels [3]. Numerous studies have shown that aberrantly expressed miRNAs in various types of cancer are associated with cell development, cell proliferation, apoptosis, and tumorigenesis [4–7].

Growing evidence has demonstrated that downregulated miR-375 expression contributes to various types of cancers. Several studies have reported that downregulated miR-375 expression was implicated in β -cell growth and glucose regulation of insulin gene expression by directly targeting PDK1 in pancreatic carcinoma [8,9]. In addition, miR-375 has been shown to inhibit cancer cell growth in liver cancer by negatively regulating oncogene AEG-1 [10]. MiR-375 is considered as an oncomiR in prostate carcinogenesis and plays a vital role in prostate cancer progression [11].

In non-small cell lung carcinoma (NSCLC), decreased miR-375 expression level was significantly correlated with lymphatic metastasis and advanced stage disease. On the contrary, high miR-375 expression could also promote cell migration and target CLDN1 in NSCLC [12]. In a previous study, miR-375 expression levels were significantly over-expressed in LUAD and small cell lung carcinoma (SCLC), whereas they were under-expressed in lung squamous cell carcinoma (LUSC) [13]. Furthermore, studies have also found that miR-375 promotes cell growth in SCLC cell lines by directly downregulating inositol-trisphosphate 3-kinase B (ITPKB) [14]. Unfortunately, data published on miR-375 expression in LUAD are partly conflicting and highly heterogeneous.

In the present study, we sought to unveil the role of miR-375 in LUAD through modulation of miRNAs expression and identification of putative molecular targets by bioinformatics analysis and analysis based on TCGA, GEO, and literature reviews.

Material and Methods

TCGA data in LUAD patients

The available data on miR-375 expression and clinical information were obtained from Illumina HiSeq Level 3 isoform quantification files available at the TCGA Data Portal website (<http://tcga.cancer.gov/dataportal>; accessed June 2016). We obtained the normalized reads per million miRNA mapped (RPM) data in 517 LUAD patients and 59 normal lung samples by summing up the raw counts. The RPM data of the miR-375 identified in this study were extracted both for 450 LUAD patients and 47 normal samples. Mean values were used for a patient with more than one portion to prevent duplicates. The LIMMA package of R language was used to identify the differentially expressed genes (DEGs) between the expression profiles of 517 LUAD patients and 59 normal samples. We identified the significance of gene expression difference by using absolute log₂ fold change (FC) >1. FDR (False Discovery Rate) of q-value was adjusted to 0.05.

Selection of GEO dataset

Next, we obtained the microarray profiles of LUAD from the GEO database (Gene Expression Omnibus, <http://www.ncbi.nlm.nih.gov/geo/>). The following keywords were used in the GEO database: (lung OR pulmonary OR respiratory OR bronchi OR bronchioles OR alveoli OR pneumocytes OR “air way”) AND (cancer OR carcinoma OR tumor OR neoplas* OR malignant* OR adenocarcinoma) AND (microRNA OR miRNA OR “micro RNA” OR “small temporal RNA” OR “noncoding RNA” OR ncRNA OR “small RNA”). The microarray datasets reporting miR-375 expression between LUAD and normal lung tissues was included in this study.

Study selection and data extraction for literature review

An electronic literature search was performed in PubMed and Web of Science (up to September 1, 2016) by using the

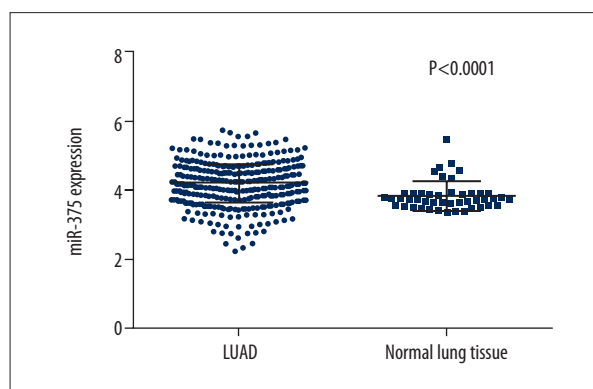


Figure 1. Expression of miR-375 in LUAD and normal lung tissues in TCGA dataset.

Table 1. Clinical covariates for the TCGA LUAD cohort.

Clinicopathological feature		n	miRNA-375 relevant expression(2 ^{-ΔCt})		
			Mean ±SD	t	P-value
Tissue	LUAD	450	14.0282±1.86840	5.542	<0.0001
	Normal lung	46	12.7962±1.38416		
Age (years)	<60	121	13.9739±1.7431	-0.156	0.876
	≥60	310	14.0050±1.9093		
Gender	Male	210	14.1536±2.0444	1.317	0.189
	Female	240	13.9185±1.6963		
Tumor stage 1	T1	154	13.8402±2.0764	1.834*	0.14
	T2	236	14.1677±1.8113		
	T3	41	13.6755±1.3020		
	T4	16	14.5330±1.7740		
Tumor stage 2	T1~2	390	14.0384±1.9244	0.46	0.646
	T3~4	57	13.9162±1.4849		
Nodes	Yes	156	14.0911±1.7676	0.501	0.616
	No	293	13.9981±1.9243		
Metastasis	Yes	159	13.9730±1.8354	-0.486	0.627
	No	287	14.0630±1.8934		
Pathologic stage 1	I	242	13.9870±1.9997	0.357*	0.784
	II	110	13.9973±1.7651		
	III	73	14.1602±1.5368		
	IV	20	14.3416±1.8340		
Pathologic stage 2	I+II	352	13.9903±1.9270	-0.962	0.337
	II+IV	93	14.1992±1.5964		
Anatomic organ subdivision	L_lower	70	14.0738±1.9777	0.985*	0.415
	L_upper	109	14.0742±1.8623		
	R_lower	85	14.1820±1.8741		
	R_middle	156	13.8154±1.8411		
	R_upper	19	14.5101±1.8248		
Location	Central	54	13.8303±1.9611	-1.03	0.305
	Peripheral	113	14.1516±1.8495		

* One-way analysis of variance (ANOVA) test was performed.

following terms: (miR-375 OR miRNA-375 OR microRNA375 OR miR375 OR miRNA375 OR miR 375 OR miRNA 375 OR microRNA 375) and (lung cancer OR lung carcinoma OR lung neoplasm OR lung tumor OR lung adenocarcinoma OR LUAD OR non-small cell lung cancer OR NSCLC). Publications were considered eligible if they met the following criteria: (1) studies

examining the expression of miR-375 in LUAD; and (2) normal lung tissues paired/unpaired used as healthy control group. The studies were considered ineligible based on the following criteria: (1) reviews, experimental studies, single case reports, meta-analyses, and conference abstracts; and (2) absence of healthy control groups.

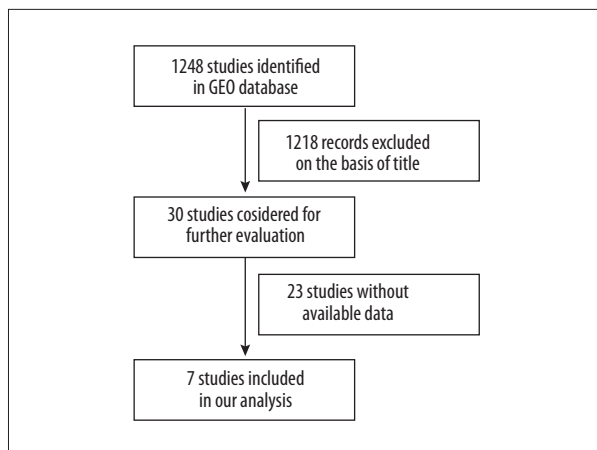


Figure 2. Flow chart of study selection for GEO dataset.

Gene ontology enrichment and target prediction analysis

The targets of miR-375 were predicted through 12 programs, including miRWALK2.0 (<http://zmf.umm.uni-heidelberg.de/apps/zmf/mirwalk2/miRretsys-self.html>). To increase the prediction accuracy, the genes were selected as targets that were overlapped in at least 5 of 12 databases (Microt4, miRWalk, mirbridge, miRanda, miRDB, miRMap, Pictar2, PITA, miRNAmap, RNAhybrid, RNA22 and Targetscan). Subsequently, we analyzed the gene overlaps integrated between DEGs in LUAD, and predicted target genes of miR-375 by bioinformatics software. Gene ontology (GO) enrichment analysis was conducted for overlapped genes by DAVID [15]. The Kyoto Encyclopedia of Genes and Genomes (KEGG) database (http://www.genome.jp/kegg/tool/search_pathway.html) was then used to map the predicted targets by using DAVID online analysis (<https://david.ncifcrf.gov/>) [16]. STRING database (the Search Tool for the Retrieval of Interacting Genes/Proteins) was also used to predict the association between miR-375 and the target gene in the regulatory network analysis [17].

Statistical analysis

All data are displayed as mean ± standard deviation (SD) from each group. Student’s *t*-test was performed to analyze the differences between two groups, whereas one-way analysis of variance (ANOVA) test was used among more than three groups. Standardized mean difference (SMD) was applied to evaluate the association between miR-375 levels and LUAD by RevMan 5.2.0 software. We pooled the SMD across GEO datasets using the Mantel-Haenszel formula (fixed-effect model) or the DerSimonian-Laird formula (random-effect model). A fixed-effect model was adopted when the Q statistic was considered significant ($p > 0.1$, or $I^2 < 50%$), otherwise, a random-effect model was used. Moreover, the relationship of DEGs expression with miR-375 level was analyzed by Spearman’s rank correlation. A two-sided *p*-value < 0.05 was considered statistically significant.

Results

MiR-375 expression in LUAD clinical tissues

The detection of MiR-375 expression in LUAD in TCGA

The expression levels of miR-375 were significantly upregulated in clinical LUAD specimens (14.0282 ± 1.86840) in comparison to adjacent non-cancerous lung tissues (12.7962 ± 1.38416 ; $p < 0.0001$, Figure 1). For all the tested parameters, no significant differences were found in the other clinical features (Table 1).

MiR-375 expression in LUAD based on GEO

Additionally, miR-375 expression was initially assessed in a series of LUAD and normal lung tissues based on GEO dataset (Figure 2). A total of seven GEO datasets (GSE40738, GSE47525, GSE48414, GSE51853, GSE74190, and GSE25508)

Table 2. Characteristics of studies based on GEO dataset.

Study	Patients			Control			t	P
	Mean	SD	n	Mean	SD	n		
GSE25508	2.2384	0.4558	5	2.2886	0.5715	5	-0.154	0.882
GSE40738	-0.5367	0.1091	45	-0.4921	0.1438	91	-1.836	0.069
GSE47525	10.3833	5.7049	6	10.4780	5.4595	14	-0.035	0.972
GSE48414	-0.0060	1.9080	154	-0.48466	0.4753	20	2.560	0.012
GSE51853	0.8610	1.9923	76	0.1738	0.2469	5	2.708	0.009
GSE63805	2.3994	0.4889	32	2.1065	0.1761	30	3.176	0.003
GSE74190	6.0000	1.8560	46	4.3600	0.8690	44	4.871	0.000
Total	SMD(95%CI)=0.33(-0.16, 0.82), P=0.18; I ² =79%, P<0.0001							

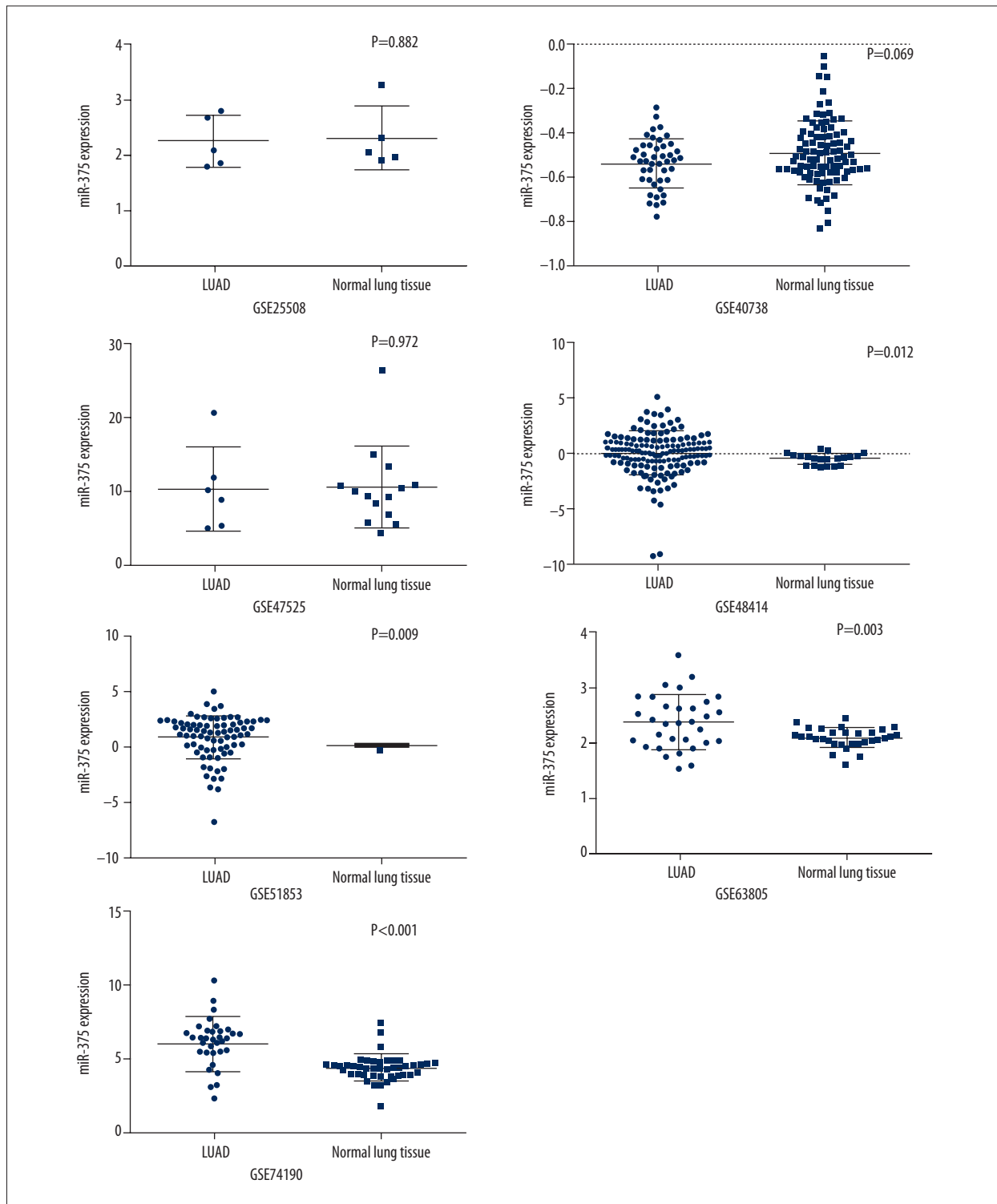


Figure 3. Expression of miR-375 in LUAD and normal lung tissues in GEO datasets.

which included both LUAD patients and healthy people, were collected in our study. The expression levels of miR-375 in LUAD tissues were significantly higher than in healthy non-cancer control tissues in GSE48414, GSE51853, GSE63805,

and GSE74190 datasets ($p=0.012$, $p=0.009$, $p=0.003$, and $p<0.0001$; respectively), whereas no significant difference was found in other GEO datasets (GSE40738, GSE47525, and GSE25508). Characteristics of studies based on GEO dataset

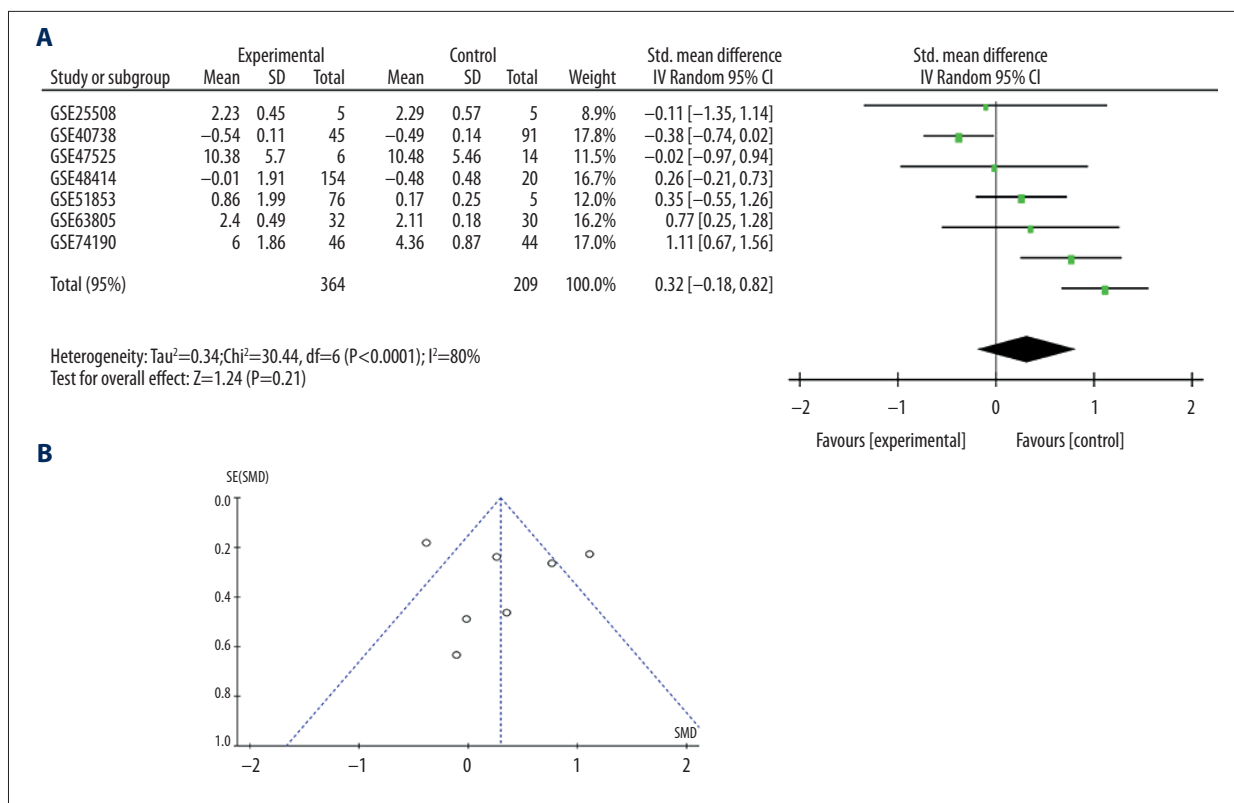


Figure 4. Forest plot (A) and funnel plot (B) of the combined SMD for miR-375 expression between LUAD and control group by the random effects models.

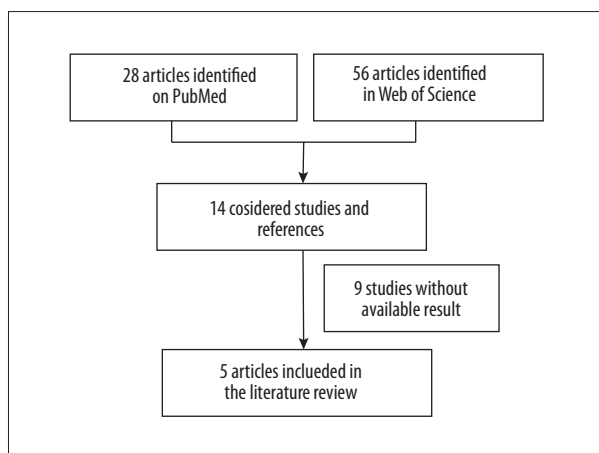


Figure 5. Flow chart of study selection for the literature review.

are presented in Table 2 and Figure 3. However, no significant difference was found between LUAD and control groups based on all the included GEO datasets (SMD=0.33; 95% CI, -0.16 to 0.82; $p=0.18$) with significant heterogeneity by random-effected model ($p<0.0001$, $I^2=79%$). The results of forest plot and funnel plot are shown in Figure 4.

Literature review of miR-375 expression profiles in LUAD versus normal lung

Next, we explored miR-375 upregulation in LUAD based on literature data. As shown in Figure 5, five studies that met the criteria for selection were selected from the literature [14,18–21]. Consistent with the result of TCGA, a common pattern of upregulation for miR-375 in LUAD were reported across the four included studies, whereas no significant upregulation was found in one study (Table 3).

MiR-375 prediction and bioinformatics analyses

Data preprocessing and DEGs screening

A total of 20,531 genes were differentially compared in LUAD TCGA data. After preprocessing, 5,817 DEGs were screened out by the difference threshold (q value <0.05 and absolute $\log_2FC >1$), including 3,843 upregulated genes and 1,794 downregulated genes. Meanwhile, 58,976 target genes for miR-375 were identified in five up-to-date prediction algorithms. Furthermore, all the 682 miR-375 predicted target genes were sorted out by language R, which were then integrated analytically between DEGs and the predicted target genes. The flow diagram and results for DEGs screening process are depicted in Figures 6 and 7.

Table 3. Overview of the 5 studies selected from literature.

Author	Year	Country	LUAD (n)	Normal lung (n)	Result	Detection methods
Yu	2010	Maryland	36	36 (paired)	Up-regulation	qRT-PCR
Hamamoto	2013	Japan	54	54 (paired)	Up-regulation	qRT-PCR
Sonia	2014	Spain	19	19 (paired)	Up-regulation	qRT-PCR
Jin	2015	China	36	44	Up-regulation	qRT-PCR
KIM	2014	Korea	35	2	NS	MicroRNA microarrays

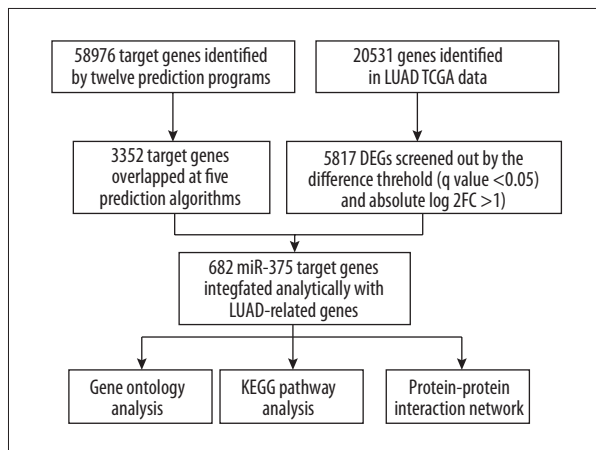


Figure 6. Flow diagram of screening for miR-375-related DEGs in LUAD.

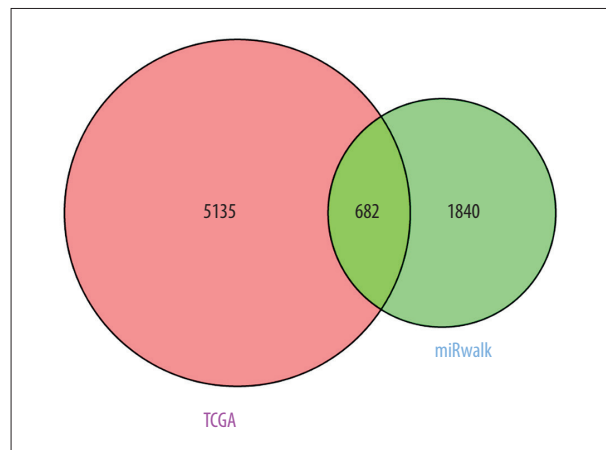


Figure 7. Venn diagram for the integration between DEGs and predicted target genes.

Functional analysis of the DEGs in lung cancer

First, we identified the functional roles of 682 potential target genes in terms of biological processes in LUAD by GO enrichment analysis. The analysis revealed that numerous target genes were involved in the biological processes, such as neuron differentiation, plasma membrane part and sequence-specific DNA binding. Then, the KEGG pathways program was used to reveal the critical pathway, in which the overrepresentation of the predicted miR-375 targets was involved, linked to carcinogenesis such as pentose and glucuronate interconversions, ascorbate and aldarate metabolism, and starch and sucrose metabolism. The top ten GO processes and KEGG pathways that were most strongly enriched with respect to miR-375 in LUAD are shown in Tables 4, 5, and Figure 8.

Protein-protein interaction network analysis

STRING was performed to construct the PPI network based on the overlapped DEGs and genes or proteins (Figure 9). In the PPI network, FGF2 (fibroblast growth factor 2), PAX6 (paired box 6), and RHOJ were revealed to exert their potential roles in LUAD by interactions with miR-375 (Table 6). The expression of

three genes were downregulated in LUAD ($\log_2FC = -2.11$, $FDR < 0.0001$; $\log_2FC = -1.431$, $FDR < 0.0001$ and $\log_2FC = -1.879$, $FDR < 0.0001$, respectively). A significant negative correlation was observed between FGF2 and miR-375 expression in LUAD patients by Spearman correlation ($r = -0.1821$, $p = 0.0001$), whereas no significant correlation was found between PAX6 and RHOJ and miR-375 ($p = 0.1221$ and $p = 0.325$, respectively; Figure 10).

Discussion

In this study, we identified the aberrantly expressed miR-375 involved in LUAD through the comparison of miRNA expression profiles in cancerous tissues with that of normal lung tissues based on validation from TCGA and GEO datasets and published studies. Additionally, we discovered novel markers and potential targets for miR-375 that were involved in the regulation of crucial biological processes in LUAD by GO analysis and KEGG pathway annotation.

To date, there have only been several studies concerning the characteristics of miR-375 in lung cancer. Li et al. were the first to demonstrate that the expression of miR-375 was lower in

Table 4. Ten processes most strongly enriched by GO analysis.

Category	Term	Count	P-value	FDR
Biological processes				
GOTERM_BP_FAT	GO: 0030182~neuron differentiation	52	1.58E-12	2.79E-09
GOTERM_BP_FAT	GO: 0048666~neuron development	44	5.76E-12	1.02E-08
GOTERM_BP_FAT	GO: 0007409~axonogenesis	32	1.39E-11	2.45E-08
GOTERM_BP_FAT	GO: 0000902~cell morphogenesis	44	2.96E-11	5.23E-08
GOTERM_BP_FAT	GO: 0048812~neuron projection morphogenesis	33	4.00E-11	7.06E-08
GOTERM_BP_FAT	GO: 0048667~cell morphogenesis involved in neuron differentiation	32	1.13E-10	1.99E-07
GOTERM_BP_FAT	GO: 0006928~cell motion	50	3.40E-10	5.99E-07
GOTERM_BP_FAT	GO: 0000904~cell morphogenesis involved in differentiation	34	3.40E-10	5.99E-07
GOTERM_BP_FAT	GO: 0048858~cell projection morphogenesis	34	3.81E-10	6.71E-07
GOTERM_BP_FAT	GO: 0032989~cellular component morphogenesis	44	9.76E-10	1.72E-06
Cellular components				
GOTERM_CC_FAT	GO: 0044459~plasma membrane part	143	3.59E-12	4.94E-09
GOTERM_CC_FAT	GO: 0005886~plasma membrane	209	1.82E-11	2.50E-08
GOTERM_CC_FAT	GO: 0031012~extracellular matrix	38	6.62E-09	9.12E-06
GOTERM_CC_FAT	GO: 0031226~intrinsic to plasma membrane	81	2.56E-07	3.52E-04
GOTERM_CC_FAT	GO: 0005578~proteinaceous extracellular matrix	33	3.60E-07	4.95E-04
GOTERM_CC_FAT	GO: 0005887~integral to plasma membrane	77	1.66E-06	0.002279
GOTERM_CC_FAT	GO: 0030054~cell junction	41	9.84E-06	0.013541
GOTERM_CC_FAT	GO: 0044421~extracellular region part	63	1.28E-05	0.017682
GOTERM_CC_FAT	GO: 0031224~intrinsic to membrane	250	1.64E-05	0.022599
GOTERM_CC_FAT	GO: 0045202~synapse	31	2.48E-05	0.034146
Molecular function				
GOTERM_MF_FAT	GO: 0043565~sequence-specific DNA binding	55	3.39E-09	5.13E-06
GOTERM_MF_FAT	GO: 0015267~channel activity	36	6.24E-06	0.00943
GOTERM_MF_FAT	GO: 0022836~gated channel activity	30	6.40E-06	0.009679
GOTERM_MF_FAT	GO: 0022803~passive transmembrane transporter activity	36	6.57E-06	0.009928
GOTERM_MF_FAT	GO: 0022838~substrate specific channel activity	35	7.55E-06	0.011411
GOTERM_MF_FAT	GO: 0003700~transcription factor activity	65	8.48E-06	0.012823
GOTERM_MF_FAT	GO: 0005216~ion channel activity	33	2.54E-05	0.038459
GOTERM_MF_FAT	GO: 0008066~glutamate receptor activity	8	1.25E-04	0.188624
GOTERM_MF_FAT	GO: 0030528~transcription regulator activity	84	2.57E-04	0.387228
GOTERM_MF_FAT	GO: 0005230~extracellular ligand-gated ion channel activity	11	3.51E-04	0.528754

Table 5. Ten KEGG pathways most strongly enriched by target genes.

Term	Input number	Background number	P-value	Corrected P-value
Pentose and glucuronate interconversions	11	36	1.99E-06	0.000464663
Ascorbate and aldarate metabolism	9	27	9.55E-06	0.001117413
Starch and sucrose metabolism	12	56	1.56E-05	0.001218749
Porphyryr and chlorophyll metabolism	10	42	3.67E-05	0.00214613
Drug metabolism – other enzymes	10	46	7.14E-05	0.002817806
Axon guidance	17	127	7.23E-05	0.002817806
Steroid hormone biosynthesis	11	58	9.26E-05	0.003093956
Retinol metabolism	11	65	0.000225	0.006578928
Protein digestion and absorption	12	90	0.000829	0.021546285
Drug metabolism – cytochrome P450	10	68	0.001135	0.0265701

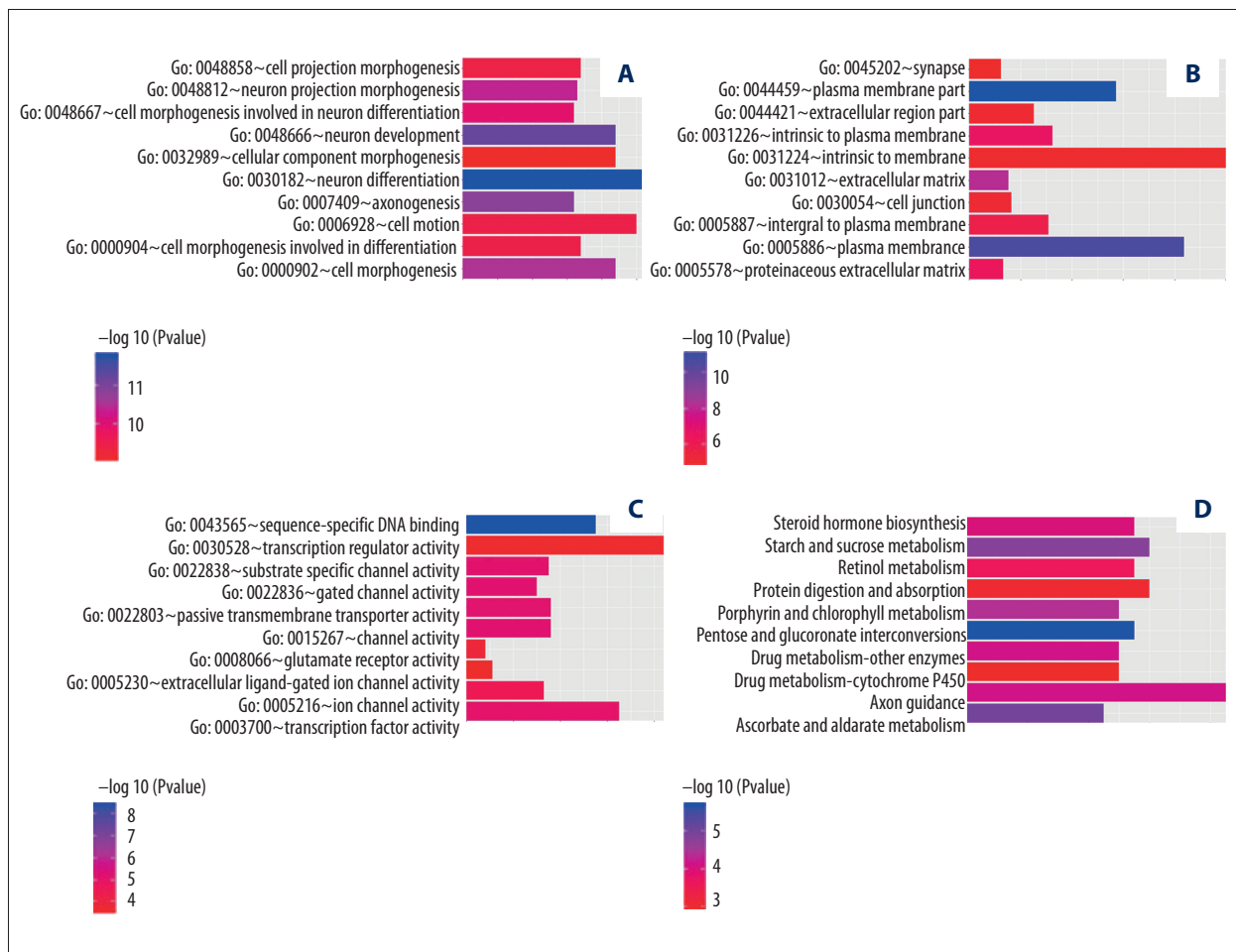


Figure 8. Top ten GO enrichment analysis (A–C) and KEGG pathways (D). (A) Biological processes; (B) cellular components; (C) molecular function; (D) KEGG pathway.

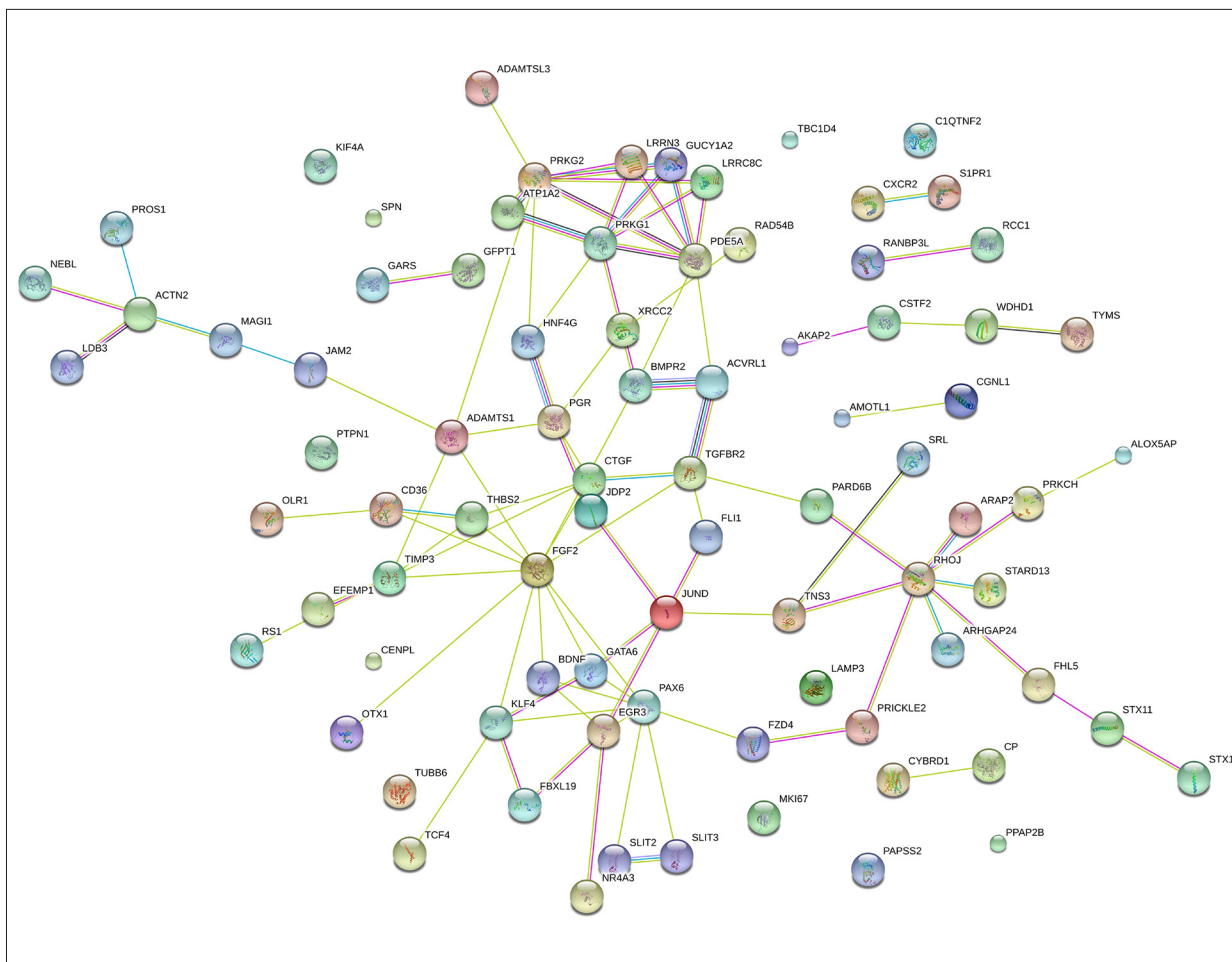


Figure 9. PPI network of new predicted LUAD-related genes.

Table 6. Top ten co-expression relationships by STRING.

Node 1	Node 2	Node 1 string internal id	Homology	Coexpression	Experimentally determined interaction	Database annotated	Automated textmining	Combined score
TGFB2	SMAD7	1853779	0	0.072	0.807	0.9	0.712	0.994
PRKG1	PDE5A	1856026	0	0.207	0.833	0	0.961	0.994
ACVRL1	TGFB2	1857773	0.77	0.077	0.857	0.9	0.809	0.988
LDB3	ACTN2	1860278	0	0.215	0.933	0	0.789	0.988
BMPR2	SMAD7	1856145	0	0.072	0.573	0.9	0.728	0.987
CENPL	CENPM	1853309	0	0	0.33	0.9	0.753	0.982
JDP2	JUND	1845956	0	0	0.874	0	0.853	0.98
WDHD1	GINS4	1854036	0	0.131	0.95	0	0.584	0.98
TCF4	TAL1	1853052	0	0	0.96	0	0.484	0.978
FZD4	WNT3	1861957	0	0	0.274	0.9	0.714	0.977

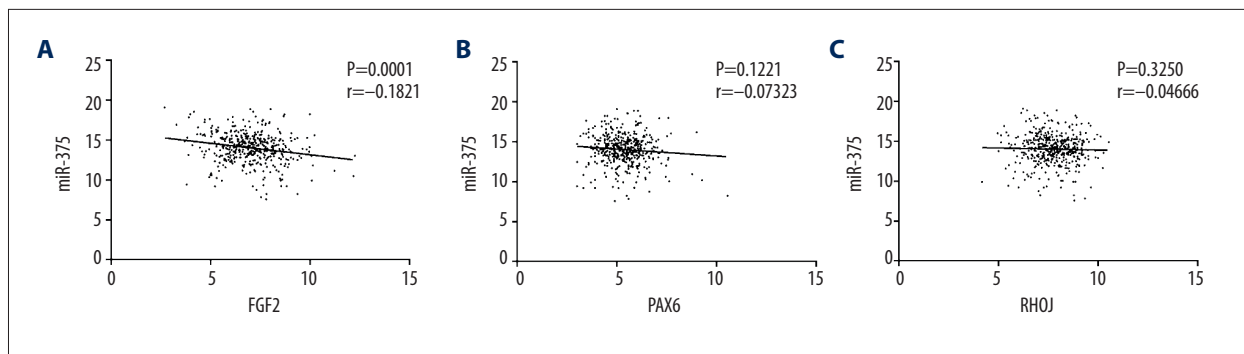


Figure 10. Relationship between miR-375 and target genes (A) FGF2; (B) PAX6; (C) RHOJ.

96 paired samples of NSCLC tissue than in matched noncancerous tissue [22]. On the contrary, Yoda et al. revealed that miR-375 was overexpressed in 54 LUAD patients as compared with normal controls by qRT-PCR [19]. Additionally, another current report on miR-375 expression in LUAD was consistent with a previous study that reported miR-375 was overexpressed in microarray profiles selected LCM cancerous cell populations derived from 36 LUADs [14]. We also found that miR-375 was constantly upregulated in LUAD tissues in TCGA data and several GEO datasets. To date, the result of the expression of miR-375 level in LUAD is still controversial, and further investigation is required to elucidate the role of miR-375 in LUAD.

Recently, it has been suggested that miR-375 targets several important genes to suppress core hallmarks of cancer, such as YAP1 (yes-associated protein), IGF1R, PDK1, and AEG-1 [9,10,23,24]. In gastric cancer, miR-375 could target PDK1 and Janus kinase 2, which consequently could reduce cell viability and suppress gastric cancer cell proliferation [25,26]. Xu et al. demonstrated that the overexpression of miR-375 remarkably suppressed consequent cell invasion and metastasis by downregulating FZD8 in colorectal cancer [27]. It was reported that AEG-1 and YAP were regulated by miR-375, and inhibited proliferation and invasion of cancer cells in hepatocellular carcinoma [10,28]. MiR-375 has been revealed to act as a tumor suppressor in human cancers, whereas it functions as an oncogene in some types of cancers. It has been shown that miR-375 overexpression facilitated cell proliferation and upregulated estrogen receptor alpha through regulation of RASD1 in breast cancer [29]. Nishikawa et al. demonstrated that miR-375 was induced by ASH1/ASCL1 in lung cancer cells, which is a key transcription factor in lung cancer with neuroendocrine features. Additionally, Yoda et al. found that high miR-375 expression promoted cell invasion and metastasis in NSCLC by targeting CLDN1 [12]. Yu et al. also found that miR-375 was consistently overexpressed in LUAD, displaying higher accuracy in diagnosis of LUAD compared with LUSC [18]. Hamaoto et al. hypothesized that miR-375 could inactivate the PI3K pathway, which is more activated in SCC than in AC [19,30]. Thus,

the molecular mechanism that is related to miR-375 overexpression in LUAD has not yet been fully elucidated.

In the present study, we identified that novel candidate target genes for miR-375 were involved in the regulation of crucial biological processes in LUAD, such as FGF2, PAX6, and RHOJ. FGF2, the most potent FGF increased in NSCLC, promotes proliferation and inhibits apoptosis of lung cancer cells. FGF2 could also promote cell malignant transformation by combining with FGFR in LUAD [31]. Interestingly, our current study revealed that FGF2 mRNA was decreased in LUAD compared with normal lung tissue. Consistent with our result, both upregulation and downregulation of FGF2 have also been detected in colorectal cancers [32,33]. As far as we know, few previous studies have indicated that the downregulated pattern of FGF2 occurs in tumor tissue compared with normal tissue. FGF2 is an important proangiogenic growth factor in the promotion of development and in tumor angiogenesis [34]. Thus, further investigation is required to explore the ectopic expression of FGF2 of LUAD cells. The transcription factor PAX6 has an oncogenic role that has different signaling pathways in different tumors. A previous study showed that PAX6 was highly expressed in lung cancer tissues and lung cancer cell lines, suggesting that PAX6 promoted the cell cycle progression in lung cancer by activating the MET tyrosine kinase receptor gene and MAPK signaling [35]. On the contrary, our study demonstrated that PAX6 mRNA expression level was stronger in normal lung tissue than in lung cancer tissue. In light of previous studies, PAX6 is also recognized as a tumor suppressor in several cancers [36–38]. PAX6 suppresses cell growth, angiogenesis, and invasiveness of glioma by inhibiting vascular endothelial growth factor A and matrix metalloproteinase-2 [39,40]. In support of the presented evidence, we hypothesize that PAX6 functioned as a tumor suppressor in LUAD. Additionally, RhoJ has been revealed to be down-expressed in LUAD, which has previously been considered as a selective and effective therapeutic target in tumor tissues. Previous studies employing animal tumor models showed that the genetic deletion of host-derived RhoJ could inhibit tumor progression and metastasis by suppressing tumor angiogenesis. Recently published studies

also demonstrated that RhoJ is involved in the progression of gastric cancer by positively regulating tumor cell motility and invasiveness. Our study was the first to report the potential role of RhoJ in LUAD. Further studies are needed to validate the therapeutic role of RhoJ in LUAD.

References:

- Siegel RL, Miller KD, Jemal A: Cancer statistics, 2016. *Cancer J Clin*, 2016; 66(1): 7–30
- Matsuda T, Machii R: Morphological distribution of lung cancer from Cancer Incidence in Five Continents Vol. X. *Jpn J Clin Oncol*, 2015; 45(4): 404
- Garzon R, Calin GA, Croce CM: MicroRNAs in cancer. *Ann Rev Med*, 2009; 60: 167–79
- Esquela-Kerscher A, Slack FJ: Oncomirs – microRNAs with a role in cancer. *Nat Rev Cancer*, 2006; 6(4): 259–69
- Wo L, Lu D, Gu X: Knockdown of miR-182 promotes apoptosis via regulating RIP1 deubiquitination in TNF-alpha-treated triple-negative breast cancer cells. *Tumour Biol*, 2016; 37(10): 13733–42
- An HJ, Kwak SY, Yoo JO et al: Novel miR-5582-5p functions as a tumor suppressor by inducing apoptosis and cell cycle arrest in cancer cells through direct targeting of GAB1, SHC1, and CDK2. *Biochim Biophys Acta*, 2016; 1862(10): 1926–37
- Hemmatzadeh M, Mohammadi H, Karimi M et al: Differential role of microRNAs in the pathogenesis and treatment of Esophageal cancer. *Biomed Pharmacother*, 2016; 82: 509–19
- Poy MN, Eliasson L, Krutzfeldt J et al: A pancreatic islet-specific microRNA regulates insulin secretion. *Nature*, 2004; 432(7014): 226–30
- Zhou J, Song S, He S et al: MicroRNA-375 targets PDK1 in pancreatic carcinoma and suppresses cell growth through the Akt signaling pathway. *Int J Mol Med*, 2014; 33(4): 950–56
- He XX, Chang Y, Meng FY et al: MicroRNA-375 targets AEG-1 in hepatocellular carcinoma and suppresses liver cancer cell growth *in vitro* and *in vivo*. *Oncogene*, 2012; 31(28): 3357–69
- Costa-Pinheiro P, Ramalho-Carvalho J, Vieira FQ et al: MicroRNA-375 plays a dual role in prostate carcinogenesis. *Clin Epigenetics*, 2015; 7: 42
- Yoda S, Soejima K, Hamamoto J et al: Claudin-1 is a novel target of miR-375 in non-small-cell lung cancer. *Lung Cancer*, 2014; 85(3): 366–72
- Huang W, Hu J, Yang DW et al: Two microRNA panels to discriminate three subtypes of lung carcinoma in bronchial brushing specimens. *Am J Respir Crit Care Med*, 2012; 186(11): 1160–67
- Jin Y, Liu Y, Zhang J et al: The expression of miR-375 is associated with carcinogenesis in three subtypes of lung cancer. *PLoS One*, 2015; 10(12): e0144187
- Dennis G Jr., Sherman BT, Hosack DA et al: DAVID: Database for annotation, visualization, and integrated discovery. *Genome Biol*, 2003; 4(5): P3
- Huang da W, Sherman BT, Lempicki RA: Systematic and integrative analysis of large gene lists using DAVID bioinformatics resources. *Nat Protoc*, 2009; 4(1): 44–57
- Szklarczyk D, Franceschini A, Wyder S et al: STRING v10: Protein-protein interaction networks, integrated over the tree of life. *Nucleic Acids Res*, 2015; 43(Database issue): D447–52
- Yu L, Todd NW, Xing L et al: Early detection of lung adenocarcinoma in sputum by a panel of microRNA markers. *Int J Cancer*, 2010; 127(12): 2870–78
- Hamamoto J, Soejima K, Yoda S et al: Identification of microRNAs differentially expressed between lung squamous cell carcinoma and lung adenocarcinoma. *Mol Med Rep*, 2013; 8(2): 456–62
- Molina-Pinelo S, Gutierrez G, Pastor MD et al: MicroRNA-dependent regulation of transcription in non-small cell lung cancer. *PLoS One*, 2014; 9(3): e90524
- Kim J, Lim NJ, Jang SG et al: miR-592 and miR-552 can distinguish between primary lung adenocarcinoma and colorectal cancer metastases in the lung. *Anticancer Res*, 2014; 34(5): 2297–302
- Li Y, Jiang Q, Xia N et al: Decreased expression of microRNA-375 in non-small cell lung cancer and its clinical significance. *J Int Med Res*, 2012; 40(5): 1662–69
- Selth LA, Das R, Townley SL et al: A ZEB1-miR-375-YAP1 pathway regulates epithelial plasticity in prostate cancer. *Oncogene*, 2016 [Epub ahead of print]
- Kong KL, Kwong DL, Chan TH et al: MicroRNA-375 inhibits tumour growth and metastasis in oesophageal squamous cell carcinoma through repressing insulin-like growth factor 1 receptor. *Gut*, 2012; 61(1): 33–42
- Tsakamoto Y, Nakada C, Noguchi T et al: MicroRNA-375 is downregulated in gastric carcinomas and regulates cell survival by targeting PDK1 and 14-3-3zeta. *Cancer Res*, 2010; 70(6): 2339–49
- Ding L, Xu Y, Zhang W et al: MiR-375 frequently downregulated in gastric cancer inhibits cell proliferation by targeting JAK2. *Cell Res*, 2010; 20(7): 784–93
- Xu L, Wen T, Liu Z et al: MicroRNA-375 suppresses human colorectal cancer metastasis by targeting Frizzled 8. *Oncotarget*, 2016; 7(26): 40644–56
- Liu AM, Poon RT, Luk JM: MicroRNA-375 targets Hippo-signaling effector YAP in liver cancer and inhibits tumor properties. *Biochem Biophys Res Commun*, 2010; 394(3): 623–27
- de Souza Rocha Simonini P, Breiling A, Gupta N et al: Epigenetically deregulated microRNA-375 is involved in a positive feedback loop with estrogen receptor alpha in breast cancer cells. *Cancer Res*, 2010; 70(22): 9175–84
- El Ouamari A, Barouk N, Martens GA et al: miR-375 targets 3'-phosphoinositide-dependent protein kinase-1 and regulates glucose-induced biological responses in pancreatic beta-cells. *Diabetes*, 2008; 57(10): 2708–17
- Li DS, Ainiwaer JL, Sheyhiding I et al: Identification of key long non-coding RNAs as competing endogenous RNAs for miRNA-mRNA in lung adenocarcinoma. *Eur Rev Med Pharmacol Sci*, 2016; 20(11): 2285–95
- Elagöz S, Egilmez R, Koyuncu A et al: The intratumoral microvessel density and expression of bFGF and nm23-H1 in colorectal cancer. *Pathol Oncol Res*, 2006; 12(1): 21–27
- Sundlisaeter E, Rosland GV, Hertel JK et al: Increased lymphatic vascular density is seen before colorectal cancers reach stage II and growth factor FGF-2 is downregulated in tumor tissue compared with normal mucosa. *APMIS*, 2009; 117(3): 212–21
- Nissen LJ, Cao R, Hedlund EM et al: Angiogenic factors FGF2 and PDGF-BB synergistically promote murine tumor neovascularization and metastasis. *J Clin Invest*, 2007; 117(10): 2766–77
- Zhao X, Yue W, Zhang L et al: Downregulation of PAX6 by shRNA inhibits proliferation and cell cycle progression of human non-small cell lung cancer cell lines. *PLoS One*, 2014; 9(1): e85738
- Zhong X, Li Y, Peng F et al: Identification of tumorigenic retinal stem-like cells in human solid retinoblastomas. *Int J Cancer*, 2007; 121(10): 2125–31
- Berkhout M, Nagtegaal ID, Cornelissen SJ et al: Chromosomal and methylation alterations in sporadic and familial adenomatous polyposis-related duodenal carcinomas. *Mod Pathol*, 2007; 20(12): 1253–62
- Shyr CR, Tsai MY, Yeh S et al: Tumor suppressor PAX6 functions as androgen receptor co-repressor to inhibit prostate cancer growth. *Prostate*, 2010; 70(2): 190–99
- Zhou YH, Hu Y, Mayes D et al: PAX6 suppression of glioma angiogenesis and the expression of vascular endothelial growth factor A. *J Neurooncol*, 2010; 96(2): 191–200
- Mayes DA, Hu Y, Teng Y et al: PAX6 suppresses the invasiveness of glioblastoma cells and the expression of the matrix metalloproteinase-2 gene. *Cancer Res*, 2006; 66(20): 9809–17

Conclusions

Altogether, the results presented here indicate that miR-375 exerts a vital role in the biology of LUAD. Further studies *in vitro* and *in vivo* are required on the mechanisms of pathogenesis to elucidate the potential role of miR-375-regulated molecular networks and gain insights into the mechanism underlying the involvement of miR-375 in LUAD.